European Radiology (2020) 30:337–345
https://doi.org/10.1007/s00330-019-06335-0

MAGNETIC RESONANCE

Native T1 mapping compared to ultrasound elastography for staging and monitoring liver fibrosis: an animal study of repeatability, reproducibility, and accuracy

Jinning Li[1] · Huanhuan Liu[1] · Caiyuan Zhang[1] · Shuyan Yang[1] · Yanshu Wang[1] · Weibo Chen[2] · Xin Li[3] · Dengbin Wang[1]

Received: 20 November 2018 / Revised: 29 May 2019 / Accepted: 19 June 2019 / Published online: 23 July 2019

Abstract

Objectives To investigate the repeatability, reproducibility, and staging and monitoring of the performance of native T1 mapping for noninvasively assessing liver fibrosis in comparison with acoustic radiation force impulse (ARFI) elastography.

Methods The repeatability and reproducibility were explored in 8 male Sprague-Dawley rats with intraclass correlation coefficient (ICC). Different degrees of fibrosis were induced in 52 rats by carbon-tetrachloride (CCl4) insult. Another 16 rats were used to build fibrosis progression and regression models. The native T1 values and shear wave velocity (SWV) were quantified by using native T1 mapping and ARFI elastography, respectively. The METAVIR system (F0–F4) was used for the staging of fibrosis. The area under the receiver operating characteristic curve (AUC) was determined to assess the performance of quantitative parameters for staging and monitoring fibrosis.

Results Native T1 values shared similar good repeatability (ICC = 0.93) and reproducibility (ICC = 0.87) with SWV (ICC = 0.84–0.93). The AUC of native T1 values were 0.84, 0.84, and 0.75 for diagnosing significant fibrosis (≥ F2) and liver cirrhosis (F4) and detecting fibrosis progression, and those of SWV were 0.81, 0.86, and 0.7, respectively. No significant difference in performance was found between the two quantitative parameters ($p \geq 0.496$). For detecting fibrosis regression, native T1 values had a better accuracy (AUC = 0.99) than SWV (AUC = 0.56; $p = 0.002$).

Conclusion Native T1 mapping may be a reliable and accurate method for noninvasively assessing liver fibrosis. Compared with ARFI elastography, it provides similar good repeatability and reproducibility, a similar high accuracy for staging fibrosis, and a better accuracy for detecting fibrosis regression.

Key Points

- *Native T1 mapping is a valuable tool for noninvasively assessing liver fibrosis and can be measured on virtually all clinical MRI machines without additional hardware or gadolinium chelate injection.*
- *Compared with acoustic radiation force impulse elastography, native T1 mapping yields similar good repeatability and reproducibility and a similar high accuracy for staging fibrosis.*
- *Native T1 mapping provides a significantly better performance for detecting fibrosis regression than acoustic radiation force impulse elastography.*

Jinning Li and Huanhuan Liu contributed equally to this work.

Electronic supplementary material The online version of this article (https://doi.org/10.1007/s00330-019-06335-0) contains supplementary material, which is available to authorized users.

✉ Dengbin Wang
wangdengbin@xinhuamed.com.cn

[1] Department of Radiology, Xinhua Hospital, Shanghai Jiao Tong University School of Medicine, No. 1665, Kongjiang Road, Shanghai 200092, China

[2] Philips Healthcare, Shanghai 200233, China

[3] GE Healthcare, Shanghai 210000, China

Keywords Magnetic resonance imaging · Elastography · Liver fibrosis · Liver cirrhosis

Abbreviations

ARFI	Acoustic radiation force impulse
AUC	Area under the receiver operating characteristic curve
CCl_4	Carbon tetrachloride
ICC	Intraclass correlation coefficient
MRE	Magnetic resonance elastography
MRI	Magnetic resonance imaging

ROI Region of interest
SWV Shear wave velocity
WsCV Within-subject coefficient of variation

Introduction

Noninvasive measurement of stiffness with magnetic resonance elastography (MRE) or ultrasound-based elastography like transient elastography and acoustic radiation force impulse (ARFI) elastography, is used for the assessment of liver fibrosis in clinical practice [1–3]. Ultrasound-based elastography is inexpensive and quick, but this method is inadequate for patients with obesity or ascites and also has sample errors [4]. MRE has a higher technical success rate and could sample the whole liver. A recent review reported that MRE had a better accuracy than ultrasound-based elastography for staging liver fibrosis [1]. However, the implementation of MRE requires an additional hardware and software. The incremental cost greatly limits its widespread use in hospitals [5].

T1 mapping, a technique which was used to quantify the longitudinal relaxation time (T1 value) of tissues, is useful for evaluating cardiac diffuse fibrosis with injection of gadolinium chelates [6, 7]. T1 mapping/T1-weighed imaging enhanced with hepatobiliary contrast agent is a surrogate imaging biomarker of liver function [8] and can be useful for the staging of liver fibrosis, however with overlap between stages, and risk of false negatives in case of impaired liver function [9]. In addition, the safety of repeated administration of gadolinium chelates should be considered [10]. Recent studies reported the potential of "native T1 mapping" (precontrast T1 mapping) for the diagnosis of liver fibrosis and as a predictor of clinical outcome in patients with chronic liver diseases [11–14]. However, we still know little about its robustness and performance for staging and monitoring fibrosis, and if its reliability and performance are similar to those of elastography.

The aim of the current study was to investigate the performance of native T1 mapping for noninvasively assessing liver fibrosis, including repeatability, reproducibility, and staging and monitoring the process of fibrosis, and to compare them with those of ARFI elastography.

Materials and methods

Animal model and study design

To decrease the influence of confounding factors, we performed this prospective study in a rat model of liver fibrosis made with carbon tetrachloride (CCl_4). All the experimental procedures were approved by the Institutional Animal Care and Use Committee of Xinhua Hospital Affiliated to Shanghai Jiao Tong University School of Medicine. A total of 76 male Sprague-Dawley rats (weight, 200 ± 20 g) were used in this study and received experimental process after 1-week adaption. All the rats were housed on a 12-h light-dark cycle with free access to standard food and water.

The flowchart of this study is shown in Fig. 1. In 8 healthy rats, native T1 mapping and ARFI elastography were performed consecutively twice in the liver on the same day in order to explore the repeatability of both modalities. A week later, the animals received the same liver imaging for the third time to investigate the reproducibility. To induce liver fibrosis with different stages, 40 rats were randomly divided into 4 groups ($n = 10$ each group) and were intraperitoneally injected with a mixture of CCl_4 and olive oil (CCl_4:olive oil = 2:3) at a dose of 1.5 ml/kg twice a week for 2, 4, 7, or 10 weeks, respectively. Control group included 12 rats receiving only pure olive oil for corresponding durations ($n = 3$ each group). As there are no approved drugs for the treatment of liver fibrosis, we adopted a common method of CCl_4 withdrawal to make the regression model of fibrosis [15]. Sixteen rats with fibrosis, induced by CCl_4 injection for 7 weeks in the same way, underwent the same magnetic resonance imaging (MRI) and ultrasound examinations (session 1). Subsequently, they were randomly divided into 2 groups ($n = 8$ each group) and received CCl_4 injection/CCl_4 withdrawal for 4 weeks to make fibrosis progress or to allow fibrotic livers regress spontaneously. The 16 rats were then performed the second liver imaging (session 2).

To avoid the acute inflammatory reaction after CCl_4 injection and spontaneous regression after CCl_4 withdrawal, the animals underwent liver imaging and subsequent liver harvesting at 3–6 days after the last insult of CCl_4. Before both imaging, animals fasted for 8–10 h and then received anesthesia with 3% barbital sodium (intraperitoneal injection at a dose of 2–3 ml/kg). To explore the variations of quantitative parameters over different locations, we performed both imaging measurements and pathological analysis respectively on the left liver lobe (left medial and/or lateral lobe) and right liver lobe (middle lobe and/or right lateral lobe and/or triangle lobe) for all rats except the 8 healthy ones in repeated measurements study, of whom only the right liver lobes were investigated.

MRI

Liver MRI was performed at a 3.0-T MRI imager (Ingenia, Philips Healthcare), using a dedicated 8-channel phased-array rat coil with a 5-cm inner diameter (Chenguang Medical Technologies Co.). Look-Locker sequence, a gradient-echo sequence with inversion recovery pulse and imaging single slice with multiphase, was used for standard transverse T1

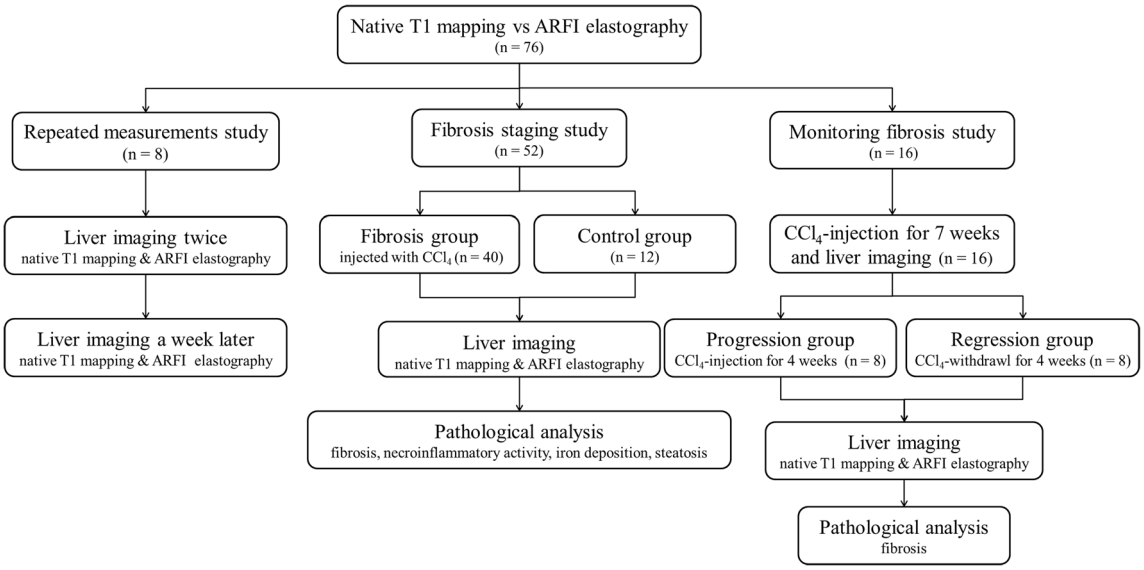

Fig. 1 Flowchart of this study. ARFI, acoustic radiation force impulse; CCl_4, carbon tetrachloride

mapping: repetition time/echo time = 5/1.7 ms, flip angle = 7°; field of view = 100 × 100 mm, matrix = 112 × 96, slice thickness = 8 mm, slice gap = 0 mm; acceleration factor = 2, number of signal averages = 1; false physiological signals used for triggering acquisitions. The methods for acquiring T1 maps and measuring native T1values are provided in Appendix E1 in the Electronic Supplementary Material. Supplementary Fig. S1 is the example of placing region of interest (ROI).

ARFI elastography

An Acuson S2000 system (Siemens Healthineers) was used to perform ARFI elastography with a 9L4 high-frequency probe. Rat hairs on the abdomen were removed with an animal shaver. The rats were then placed on a mounting plate. A sonographer (S.L.G., with 5-year experience in liver ARFI elastography) who was blinded to the MRI and pathological results measured the shear wave velocity (SWV) of rat livers in supine position. A ROI of 5 × 6 mm^2 was placed in the liver parenchyma at the depth of 0.7–1.5 cm from the liver capsule, free from large blood vessels, artifacts, and obvious acoustic shadows. The mean SWV calculated from 10 ROIs was recorded respectively for the left and right liver lobes.

Pathology

Following imaging experiment, the rats were sacrificed by cervical dislocation after deep anesthesia with intraperitoneal injection of barbital sodium. Liver samples were formaldehyde-fixed, embedded in paraffin, cut into serial sections with a thickness of 4 μm, and then stained with hematoxylin-eosin, Sirius red, and Prussian blue. A pathologist (X.Y.W., with 16 years of experience in liver pathology), blinded to the results of MRI and ultrasound, evaluated the degree of fibrosis (F0–F4) and necroinflammatory activity (A0–A3) based on the METAVIR classification system: F0 = no fibrosis, F1 = mild fibrosis (portal fibrosis without septa), F2 = substantial fibrosis (periportal fibrosis and few septa), F3 = advanced fibrosis (numerous septum fibroses without cirrhosis), F4 = cirrhosis (widespread fibrosis); A0 = absent, A1 = mild activity, A2 = moderate activity, A3 = severe activity. Liver fibrosis (≥ F2) was recognized as a significant fibrosis. Iron deposition in the liver was scored as follows: 0 = none, 1 = minimal, 2 = mild, 3 = moderate, 4 = severe [16]. The involvement of steatosis was graded from 0 to 3: 0, < 5%; 1, 5–33%; 2, > 33–66%; 3, > 66%.

Statistics

Intraclass correlation coefficient (ICC) and within-subject coefficient of variation (WsCV) were calculated to evaluate the repeatability (ICC-1, WsCV-1) and reproducibility (ICC-2, WsCV-2) of native T1 values and SWV. Correlations among native T1 value, SWV, and the stage of fibrosis were analyzed with Spearman's rank correlation. Mixed model analysis of variance with Bonferroni's correction was used to compare the quantitative values (native T1 values and SWV) between different lobes and different degrees of pathological changes (fibrosis, necroinflammatory activity, iron deposition, and steatosis). As detecting significant liver fibrosis (≥ F2) and cirrhosis (F4) is of significant importance for the treatment, receiver operating characteristic curves and AUCs were used to evaluate the corresponding performance of native T1 mapping and ARFI elastography. The cutoff values, diagnostic sensitivity, and specificity were determined based on Youden's index. Nonparametric Wilcoxon's test and the Mann–Whitney *U* test were used to compare the quantitative parameters (native T1 values and SWV) between different

Table 1 Repeatability and reproducibility of native T1 mapping and ARFI elastography

Parameters	ICC-1	WsCV-1 (%)	ICC-2	WsCV-2 (%)
Native T1 value	0.93	1.54	0.87	1.87
95% confidence interval	0.63–0.99		0.34–0.97	
p	0.001		0.008	
SWV	0.93	4.13	0.84	6.6
95% confidence interval	0.65–0.99		0.22–0.97	
p	0.001		0.013	

ICC intraclass correlation coefficient, *WsCV* within-subject coefficient of variation, *SWV* shear wave velocity

groups (progression group vs. regression group) and sessions (session 1 vs. session 2). Receiver operating characteristic curves and AUCs were also adopted to evaluate the performance of quantitative parameters for detecting the progression/regression of fibrosis. Receiver operating characteristic curves were compared with DeLong's test. Statistical analyses were conducted with SPSS statistics software (v. 23, IBM) and MedCalc (v. 11.4.2.0). p values were reported with two sides, and $p < 0.05$ was considered to be statistically significant.

Results

Animal models and pathological results

All 8 healthy rats completed the study of repeated measurements. In fibrosis staging study, 2 and 3 rats died of hepatotoxicity or anesthetic accidents in groups receiving CCl_4 injection for 7 and 4 weeks, respectively. A total of 94 liver samples from 47 rats were acquired for pathological evaluation, and the stages of fibrosis were as follows: F0, 27 (left, 13; right, 14); F1, 11 (left, 4; right, 7); F2, 17 (left, 10; right, 7); F3, 23 (left, 12; right, 11); F4, 16 (left, 8; right, 8). Among them, 21.28% rats (10/47) showed a one-stage difference in fibrosis between the left and right liver lobes, and the others (37/47) had no inter-lobe difference. There is no statistical significance for the fibrosis stages between the two lobes ($p = 0.058$). For necroinflammatory activity, 51 (left, 25; right, 26), 41 (left, 21; right, 20), 2 (left, 1; right, 1), and 0 specimens were respectively diagnosed as A0–A3. There was 76 (left, 36; right, 40), 18 (left, 11; right, 7), 0, and 0 liver samples diagnosed as 0–3 for iron deposition, respectively. Steatosis content was scored as 0–3 respectively in 72 (left, 36; right, 36), 22 (left, 11; right, 11), 0, and 0 liver samples. The results of fibrosis stages for fibrosis progression and regression group were shown in Appendix E2 in the Electronic Supplementary Material. There was a significant difference in the fibrosis stages between the two groups ($p = 0.002$).

Repeatability and reproducibility

The ICCs and WsCVs of native T1 values and SWV are summarized in Table 1. Similar good repeatability was observed for both parameters, while the reproducibility was demonstrated relatively poor. However, native T1 values seemed to always have slightly lower variations during repeated measurements than SWV.

Staging liver fibrosis

As illustrated in Supplementary Fig. S2, native T1 values (rho = 0.69, $p < 0.001$) and SWV (rho = 0.64, $p < 0.001$) demonstrated similar moderate correlations with the stages of fibrosis. There was also a moderate correlation between native T1 values and SWV (rho = 0.62, $p < 0.001$). Figures 2 and 3 displayed that both quantitative values increased significantly with the advance of fibrosis stage ($p < 0.001$). Significant differences were observed for both parameters (Fig. 3) between F0–1 and F2–4 (native T1 value, $p = 0.009$; SWV, $p = 0.002$) and between F0–3 and F4 (native T1 value, $p = 0.001$; SWV, $p < 0.001$). Besides, both quantitative parameters measured in the right lobe were significantly higher than those in the left lobe ($p < 0.001$), as depicted in Fig. 3. Figure 4 and Table 2 displayed that native T1 values manifested the same high accuracy (AUC = 0.84) for diagnosing significant fibrosis (≥ F2) and liver cirrhosis (F4), while SWV presented a higher accuracy for diagnosing liver cirrhosis (F4, AUC = 0.86) than significant fibrosis (≥ F2, AUC = 0.81). The performance between the two parameters had no significant difference for staging fibrosis (≥ F2, $p = 0.496$; F4, $p = 0.732$). In this study, there is no significant difference in native T1 values among livers with different degrees of necroinflammation ($p = 0.315$), iron deposition ($p = 0.08$), and steatosis ($p = 0.157$), while a significant difference in SWV was found between the livers having different grades of steatosis (steatosis, $p = 0.017$; necroinflammation, $p = 0.136$; iron deposition, $p = 0.57$).

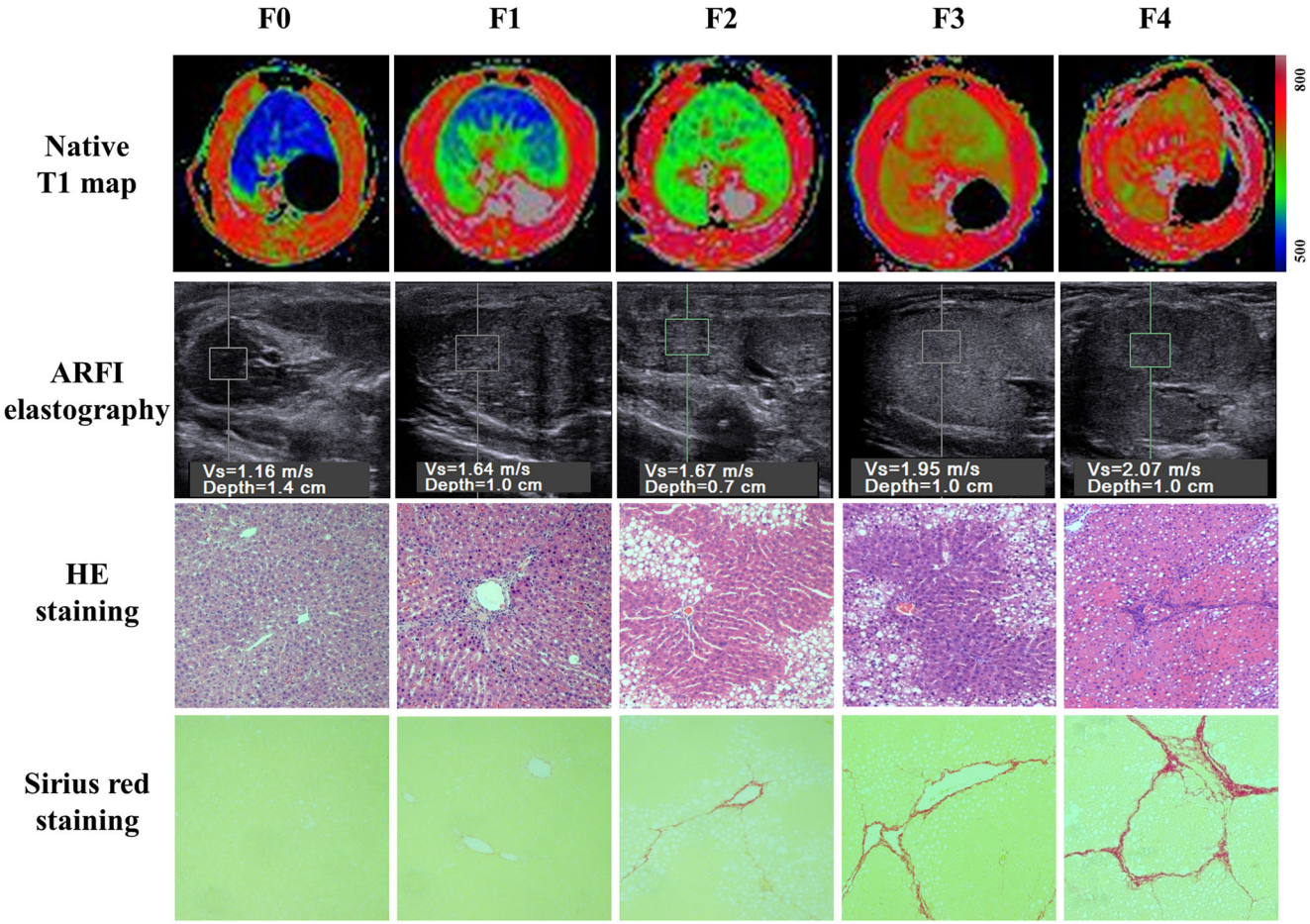

Fig. 2 Color-coded native T1 maps and acoustic radiation force impulse (ARFI) images in the liver and the hematoxylin-eosin (HE) and Sirius red staining (× 100) of liver specimens at F0–F4 stages. Both native T1 values (from blue gradually to green and then to red) and SWV increased with the advance of fibrosis stage

Monitoring liver fibrosis

As illustrated in Figs. 5 and 6, both native T1 values and SWV increased significantly after the progression of liver fibrosis ($p \leq 0.041$), while only native T1 values decreased significantly after the regression of liver fibrosis ($p = 0.002$). Table 3 summarizes the diagnostic performance of both values for detecting fibrosis progression and regression in the liver.

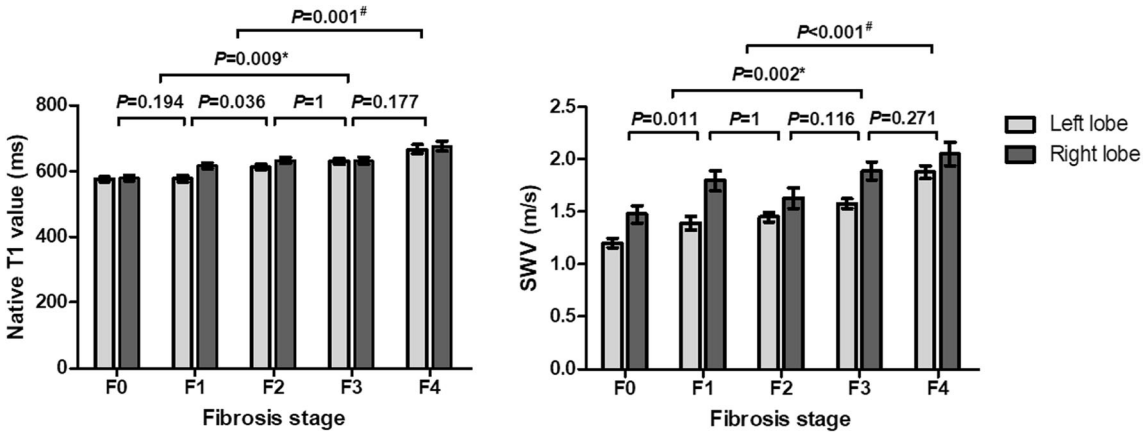

Fig. 3 Native T1 values and shear wave velocity (SWV) of F0–F4 liver fibrosis measured at the left and right liver lobes. All the values increased significantly with the advance of fibrosis stage ($p < 0.001$). Furthermore, both native T1 values and SWV measured in the right liver lobe were higher than those in the left lobe ($p < 0.001$), which was more significant for SWV values. *A comparison of quantitative parameters between F0–F1 and F2–4. #A comparison of quantitative parameters between F0–F3 and F4

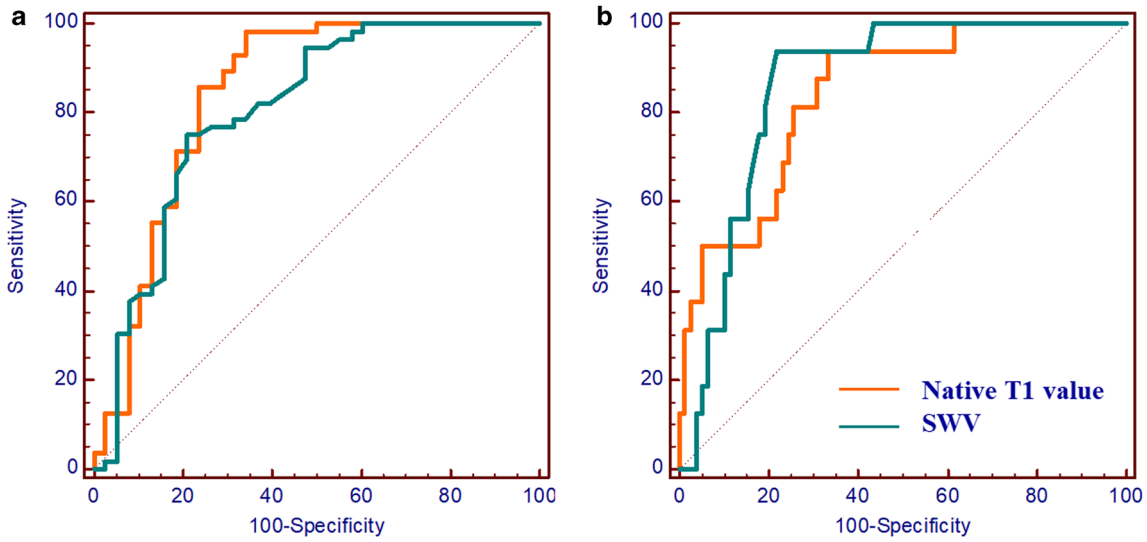

Fig. 4 Receiver operating characteristic curves of native T1 values and shear wave velocity (SWV) for diagnosing (**a**) significant fibrosis (≥ F2) and (**b**) cirrhosis (F4) in the liver

Compared with SWV, native T1 values had a similar high accuracy for detecting fibrosis progression ($p = 0.662$) and a significantly higher accuracy for detecting fibrosis regression ($p = 0.002$).

Discussion

The results of this study suggest that native T1 mapping is a reliable, accurate, and noninvasive tool for assessing liver fibrosis in rodents and possibly also in humans. Native T1 mapping was as robust as ARFI elastography through repeated measurements. For assessing liver fibrosis, it provided a similar high accuracy for staging fibrosis (≥ F2 and F4) and detecting fibrosis progression and also yielded a higher accuracy than ARFI elastography for detecting fibrosis regression.

Previous studies also showed an excellent agreement through repeated liver examinations for native T1 mapping (coefficient of variation, 1.3–1.8%) [13] and ARFI elastography (ICC, 0.85–0.89) [17]. Both our results and meta-analysis demonstrate a trend of ARFI elastography towards a better value for diagnosing high-stage fibrosis and liver cirrhosis [18, 19]. The reported AUCs were 0.82, 0.85, 0.94, and 0.94 for diagnosing fibrosis of ≥ F1, ≥ F2, ≥ F3, and F4, respectively [18]. In contrast, as our results and previous studies revealed, native T1 mapping seemed to provide a similar or even better performance for diagnosing early-stage fibrosis. In a study including 79 patients with various liver diseases, the AUC of native T1 mapping for diagnosing liver fibrosis (≥ F1) was 0.94 [13]. For staging liver fibrosis, the AUCs were 0.803, 0.712, and 0.696, respectively, for diagnosing ≥ F1, ≥ F2, and F3 liver fibrosis in another animal study [20]. Therefore, native T1 mapping might be a better choice for detecting an early-stage fibrosis than ARFI elastography. To the best of our knowledge, now, there is no study that has investigated the usefulness of native T1 mapping for evaluating the regression of liver fibrosis,

Table 2 Performance of native T1 mapping and ARFI elastography for diagnosing significant liver fibrosis (≥ F2) and cirrhosis (F4)

	AUC	95% confidence interval	Cutoff values	Sensitivity (%)	Specificity (%)	*p**
≥ F2						
Native T1 value	0.84	0.75–0.91	577.95 ms	98.21	65.79	0.496
SWV	0.81	0.71–0.88	1.54 m/s	75	78.95	
F4						
Native T1 value	0.84	0.75–0.91	617.98 ms	93.75	66.67	0.732
SWV	0.86	0.78–0.92	1.71 m/s	93.75	78.21	

*A comparison of receiver operating characteristic curves between native T1 value and SWV with DeLong's test. *AUC* area under the receiver operating characteristic curve, *SWV* shear wave velocity

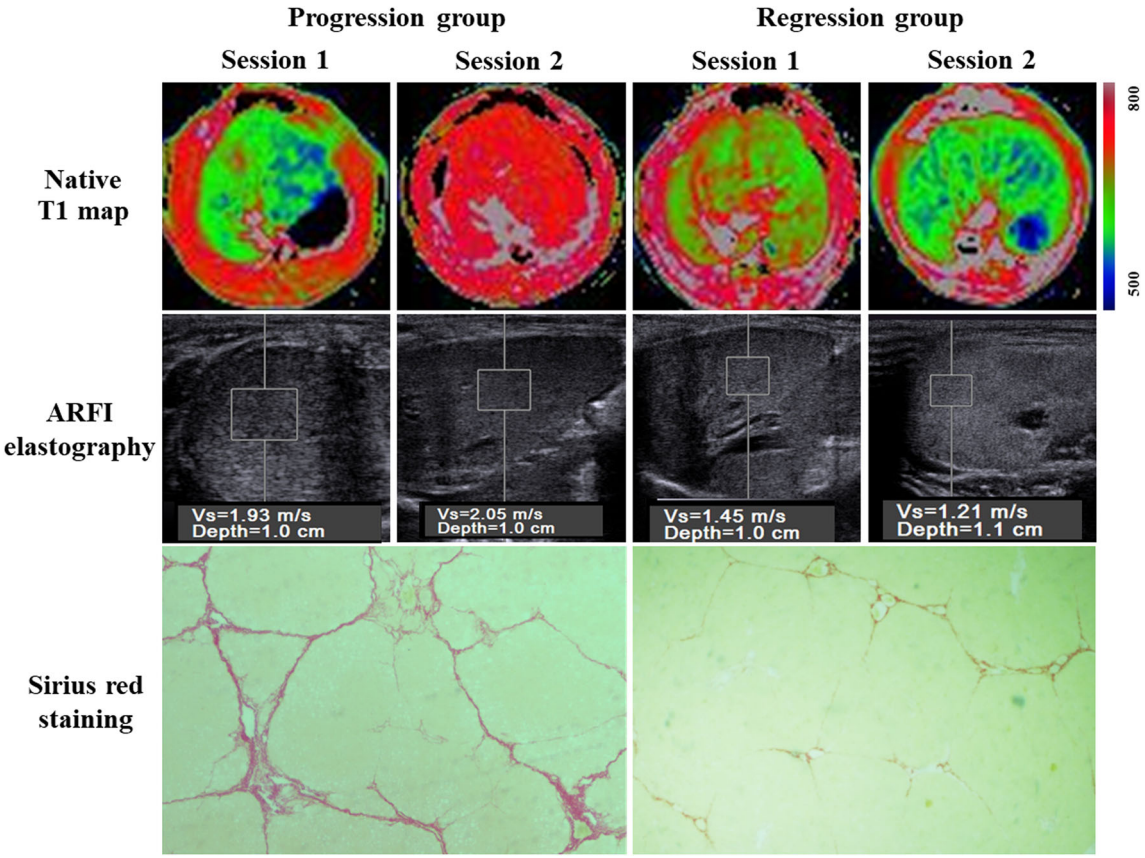

Fig. 5 Color-coded native T1 maps, acoustic radiation force impulse (ARFI) images, and the Sirius red staining (× 40) of liver specimens in the fibrosis progression/regression groups. The images vividly depicted that both native T1 values and shear wave velocity (SWV) increased after the progression of liver fibrosis and decreased after the regression of fibrosis

and even further compared it with any modality of elastography. The reason for the superiority of native T1 mapping over ARFI elastography for detecting fibrosis regression is still unclear, and further studies are needed.

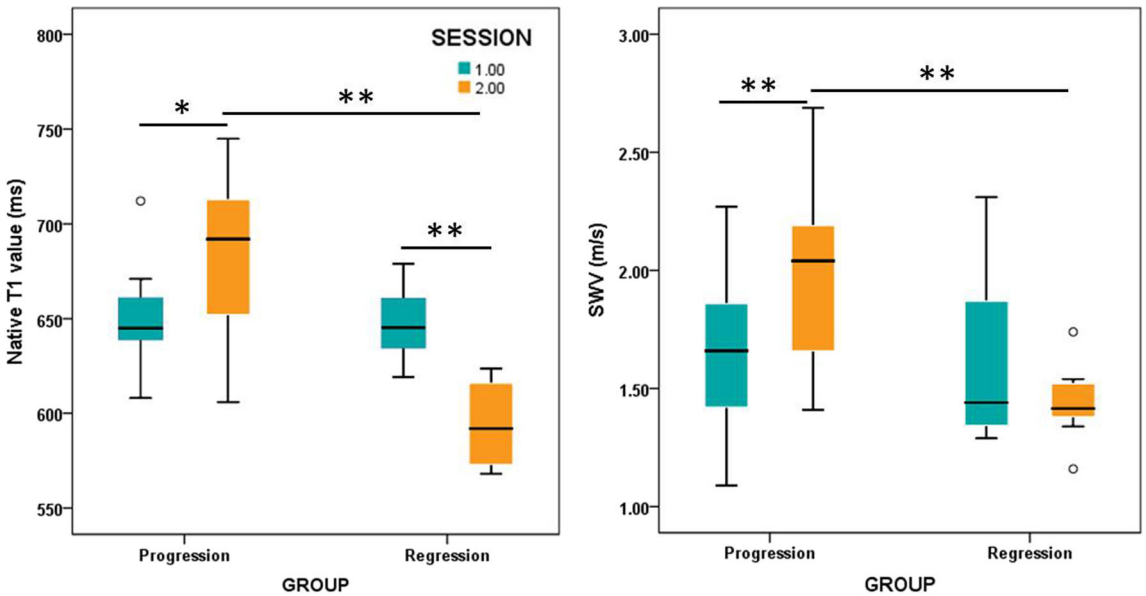

Fig. 6 Box plots of native T1 values and shear wave velocity (SWV) in the progression and regression groups of liver fibrosis. Both quantitative parameters increased significantly after the progression of liver fibrosis ($p \leq 0.041$); however, only native T1 values decreased significantly after the regression of fibrosis ($p = 0.002$). *$p < 0.05$, **$p < 0.01$

Table 3 Performance of native T1 mapping and ARFI elastography for detecting fibrosis progression and regression in the liver

	AUC	95% confidence interval	Cutoff value	Sensitivity (%)	Specificity (%)	*p**
Progression						
Native T1 value	0.75	0.55–0.89	670.92 ms	71.43	92.86	0.662
SWV	0.7	0.5–0.86	1.61 m/s	85.71	50	
Regression						
Native T1 value	0.99	0.83–1	623.66 ms	100	91.67	0.002
SWV	0.56	0.34–0.76	1.74 m/s	100	41.67	

*A comparison of receiver operating characteristic curves between native T1 value and SWV with DeLong's test. *AUC* area under the receiver operating characteristic curve, *SWV* shear wave velocity

Pathologically, the left and right liver lobes presented similar stages of fibrosis, while both native T1 values and SWV measured at different lobes were significantly different. This inter-lobe difference has been reported by previous studies for ARFI elastography, but has not been investigated for native T1 mapping [21, 22]. The cause of this phenomenon is unknown and should be further investigated. One consequence is that when pathology is the standard reference, native T1 values should be measured in the area where the biopsy is performed and not in the whole liver or the other lobe. Additionally, measurement of native T1 values varies with the field strength. As a consequence, follow-up of native T1 mapping in longitudinal studies should be performed on machines with the same field strength to keep comparability.

Although collagen deposition is the only significant influencing factor for the measurement of native T1 values in this experimental study, other pathological changes in the liver (e.g., inflammation, iron concentration, and steatosis) could act as confounding factors and influence the measurement [23, 24]. In human studies, native T1 value increases in patients with hepatic inflammation due to the elevated water content, while it is reduced in the case of iron deposition [25, 26]. As fibrosis is always accompanied with the above pathological changes in chronic liver diseases, native T1 mapping used alone may inevitably lose some accuracy for evaluating fibrosis in patients. However, it could be combined and corrected with other MRI parameters (e.g., proton density fat fraction and T2* value), which could accurately quantify the confounding factors (e.g., steatosis or iron deposition) and improve its performance for estimating fibrosis [13].

MRE has been proposed as the most accurate imaging technique for staging liver fibrosis (AUC, 0.87–0.93) by head-to-head studies, especially for patients with ascites or obesity [27, 28]. Recent studies also found that enhanced T1 mapping with gadoxetic acid is strongly correlated ($r = 0.96$, $p < 0.001$) with the severity of liver fibrosis [8] and has a high accuracy (AUC, 0.81–0.85) for staging fibrosis [9]. The advantage of native T1 mapping is that implementation does not need additional hardware or contrast agent. It could be applied in almost every MR machine without extra cost, ensuring a wide availability. T1 mapping is a quick sequence. As multiparametric MRI develops for evaluating diffuse liver diseases, availability and quick acquisition are clear advantages, favoring native T1 mapping [14].

There are several limitations in this study. First, the degree of inflammation, iron deposition, and steatosis was too minimal to explore their confounding effect on the measurement of native T1 values and SWV. Second, since the important value of MRE has been widely acknowledged for assessing liver fibrosis, the comparison of native T1 mapping with MRE would be desirable, but was not included in this study because of the unavailability of MRE in our hospital. Third, this study evaluated liver fibrosis in a rat model made with CCl_4. Generalization to patients with fibrosis of different origins needs to be tested.

In conclusion, our study demonstrates that native T1 mapping is a noninvasive, reliable, and accurate imaging method for assessing experimental liver fibrosis in rodents. As compared with ultrasound elastography, it provides similar good repeatability and reproducibility, a similar high accuracy for staging fibrosis, and a significant better accuracy for detecting fibrosis regression.

Acknowledgments We thank Dr. Shengli Gu, Department of Ultrasound, for performing the ARFI elastography on livers of rats and Dr. Xiaoying Wang, Department of Pathology (Xinhua Hospital), for pathological analysis of liver specimens. We are also grateful to Xi Zhang, PhD (Clinical Research Unite, Xinhua Hospital, Shanghai Jiao Tong University School of Medicine, Shanghai, China), for her statistical support of this study.

Funding This work was supported by the fund of National Natural Science Foundation of China (NSFC No. 81371621), Shanghai Shenkang Hospital Development Center (No. SHDC 22015022), and Shanghai Municipal Planning Commission of Science and Research Fund (201640143). The funders had no role in the study design, data collection and analysis, decision to publish, or preparation of the manuscript.

Compliance with ethical standards

Guarantor The scientific guarantor of this publication is Dengbin Wang, MD, PhD, the chief of the Department of Radiology, Xinhua Hospital Affiliated to Shanghai Jiao Tong University School of Medicine.

Conflict of interest The authors of this manuscript declare no relationships with any companies, whose products or services may be related to the subject matter of the article.

Statistics and biometry We have consulted an expert in statistics (Xi Zhang, PhD, Clinical Research Unite, Xinhua Hospital, Shanghai Jiao Tong University School of Medicine, Shanghai, China).

Informed consent All experimental procedures were approved by the Institutional Animal Care and Use Committee of Xinhua Hospital Affiliated to Shanghai Jiao Tong University School of Medicine.

Methodology
- prospective
- experimental study
- performed at one institution

References

1. Petitclerc L, Sebastiani G, Gilbert G, Cloutier G, Tang A (2017) Liver fibrosis: review of current imaging and MRI quantification techniques. J Magn Reson Imaging 45:1276–1295
2. Zhuang Y, Ding H, Zhang Y, Sun H, Xu C, Wang W (2017) Two-dimensional shear-wave elastography performance in the noninvasive evaluation of liver fibrosis in patients with chronic hepatitis B: comparison with serum fibrosis indexes. Radiology 283:873–882
3. Friedrich-Rust M, Wunder K, Kriener S et al (2009) Liver fibrosis in viral hepatitis: noninvasive assessment with acoustic radiation force impulse imaging versus transient elastography. Radiology 252:595–604
4. Tsochatzis EA, Gurusamy KS, Ntaoula S, Cholongitas E, Davidson BR, Burroughs AK (2011) Elastography for the diagnosis of severity of fibrosis in chronic liver disease: a meta-analysis of diagnostic accuracy. J Hepatol 54:650–659
5. Talwalkar JA, Yin M, Fidler JL, Sanderson SO, Kamath PS, Ehman RL (2008) Magnetic resonance imaging of hepatic fibrosis: emerging clinical applications. Hepatology 47:332–342
6. Taylor AJ, Salerno M, Dharmakumar R, Jerosch-Herold M (2016) T1 mapping: basic techniques and clinical applications. JACC Cardiovasc Imaging 9:67–81
7. Germain P, El Ghannudi S, Jeung MY et al (2014) Native T1 mapping of the heart - a pictorial review. Clin Med Insights Cardiol 8:1–11
8. Sheng RF, Wang HQ, Yang L et al (2017) Assessment of liver fibrosis using T1 mapping on Gd-EOB-DTPA-enhanced magnetic resonance. Dig Liver Dis 49:789–795
9. Feier D, Balassy C, Bastati N, Stift J, Badea R, Ba-Ssalamah A (2013) Liver fibrosis: histopathologic and biochemical influences on diagnostic efficacy of hepatobiliary contrast-enhanced MR imaging in staging. Radiology 269:460–468
10. Nehra AK, McDonald RJ, Bluhm AM et al (2018) Accumulation of gadolinium in human cerebrospinal fluid after gadobutrol-enhanced MR imaging: a prospective observational cohort study. Radiology 288:416–423
11. Ramachandran P, Serai SD, Veldtman GR et al (2019) Assessment of liver T1 mapping in fontan patients and its correlation with magnetic resonance elastography-derived liver stiffness. Abdom Radiol (NY) 44(7):2403–2408
12. Ostovaneh MR, Ambale-Venkatesh B, Fuji T et al (2018) Association of Liver Fibrosis With Cardiovascular Diseases in the General Population: The Multi-Ethnic Study of Atherosclerosis (MESA). Circ Cardiovasc Imaging 11 (3)
13. Banerjee R, Pavlides M, Tunnicliffe EM et al (2014) Multiparametric magnetic resonance for the non-invasive diagnosis of liver disease. J Hepatol 60:69–77
14. Pavlides M, Banerjee R, Sellwood J et al (2016) Multiparametric magnetic resonance imaging predicts clinical outcomes in patients with chronic liver disease. J Hepatol 64:308–315
15. Zhao F, Wang YX, Yuan J et al (2012) MR T1rho as an imaging biomarker for monitoring liver injury progression and regression: an experimental study in rats with carbon tetrachloride intoxication. Eur Radiol 22:1709–1716
16. Deugnier Y, Turlin B (2011) Pathology of hepatic iron overload. Semin Liver Dis 31:260–271
17. Balakrishnan M, Souza F, Muñoz C et al (2016) Liver and spleen stiffness measurements by point shear wave elastography via acoustic radiation force impulse: intraobserver and interobserver variability and predictors of variability in a US population. J Ultrasound Med 35:2373–2380
18. Guo Y, Parthasarathy S, Goyal P, McCarthy RJ, Larson AC, Miller FH (2015) Magnetic resonance elastography and acoustic radiation force impulse for staging hepatic fibrosis: a meta-analysis. Abdom Imaging 40:818–834
19. Hu X, Qiu L, Liu D, Qian L (2017) Acoustic radiation force impulse (ARFI) elastography for noninvasive evaluation of hepatic fibrosis in chronic hepatitis B and C patients: a systematic review and meta-analysis. Med Ultrason 19:23–31
20. Li Z, Sun J, Hu X et al (2016) Assessment of liver fibrosis by variable flip angle T1 mapping at 3.0T. J Magn Reson Imaging 43:698–703
21. Toshima T, Shirabe K, Takeishi K et al (2011) New method for assessing liver fibrosis based on acoustic radiation force impulse: a special reference to the difference between right and left liver. J Gastroenterol 46:705–711
22. Diaz S, Mostafavi B, Tanash HA, Piitulainen E (2018) Acoustic radiation force impulse (ARFI) elastography in a cohort of alpha-1 antitrypsin-deficient individuals and healthy volunteers. Acta Radiol Open 7:2058460118768363
23. Dekkers IA, Lamb HJ (2018) Clinical application and technical considerations of T1 & T2(*) mapping in cardiac, liver, and renal imaging. Br J Radiol 91:20170825
24. Unal E, Idilman IS, Karçaaltıncaba M (2017) Multiparametric or practical quantitative liver MRI: towards millisecond, fat fraction, kilopascal and function era. Expert Rev Gastroenterol Hepatol 11:167–182
25. Henninger B, Kremser C, Rauch S et al (2012) Evaluation of MR imaging with T1 and T2* mapping for the determination of hepatic iron overload. Eur Radiol 22:2478–2486
26. Hoad CL, Palaniyappan N, Kaye P et al (2015) A study of T(1) relaxation time as a measure of liver fibrosis and the influence of confounding histological factors. NMR Biomed 28:706–714
27. Cui J, Heba E, Hernandez C et al (2016) Magnetic resonance elastography is superior to acoustic radiation force impulse for the diagnosis of fibrosis in patients with biopsy-proven nonalcoholic fatty liver disease: a prospective study. Hepatology 63:453–461
28. Park CC, Nguyen P, Hernandez C et al (2017) Magnetic resonance elastography vs transient elastography in detection of fibrosis and noninvasive measurement of steatosis in patients with biopsy-proven nonalcoholic fatty liver disease. Gastroenterology 152:598–607 e592